MULTI-SQUINT ANALYSIS TO SEPARATE GEOMETRIC AND ATMOSPHERIC PHASE ARTIFACTS IN SPACEBORNE INSAR

Simone Mancon [(1)], Andrea Monti Guarnieri [(1)], Stefano Tebaldini [(1)], Davide Giudici [(2)]

[(1)] *Politecnico di Milano, Piazza Leonardo da Vinci, 32, 20133 Milano, Italy*
[(2)] *Aresys, Via Bistolfi, 49, 20134 Milano, Italy*

ABSTRACT

The main issue during phase calibration of spaceborne SAR system is to properly identify and separate different contributions to the interferometric phase. In this paper we suggest to exploit the Multi-Squint (MS) interferometric phase in order to remove InSAR fringes due to a linear orbital error, under the key assumption that the MS phase is very poorly affected by contributions from the atmospheric delay. Preliminary results obtained by processing TerraSAR-X stripmap data appear to confirm the validity of this assumption, and suggest that MS processing can be operationally employed for the calibration of spaceborne InSAR data-stacks.

1. INTRODUCTION

Data acquired by modern spaceborne synthetic aperture radar (SAR) systems are usually provided with orbital state vectors which provide the sensor position with a precision of a few centimeters. Precise orbit information for the ERS-1, ERS-2, and ENVISAT are obtained by jointly exploiting several measures (gyroscopes, laser ranging, altimeters, etc.) and orbit gravitational models [1]. More recent spaceborne SAR systems (such as COSMO-SkyMed [2] and TerraSAR-X (TSX) [3]) are equipped with GPS receivers. In particular the best TSX orbit product, the science orbits, is obtained by processing various auxiliary data, like GPS ephemerides, attitude information from the satellite's star sensors and physical model parameters. A daily science orbit arc is computed exploiting also 3 hours of overlap with the previous and the following day [3].

Still, the InSAR phase is very sensitive even to small orbital error (a few millimeters) in the parallel baseline direction.

The problem of the baseline error was already widely treated in literature concerning airborne SAR systems [4][5], where the geometrical error is usually more critical. Concerning spaceborne SAR systems, [6] and [7] describe InSAR phase artifacts due to orbital errors on RADARSAT and ERS respectively. Those methods use the InSAR phase to estimate the orbital error, although they generally cannot distinguish atmospheric phase screen (APS) from the orbital error contribution. We note that this limit does not apply if interferometry is performed with two acquisition of the scene that share the round-trip path and if they are separated by a lapse of time in which the atmosphere can be considered

constant [8]. We propose in this paper to exploit squint angle diversity to recover some satellite orbit errors. Thanks to the link between azimuth frequency and the geometrical squint angle, the MS analysis is comparable to an interferometry performed with two acquisition separated by a very small lapse of time (less than 0.5 seconds) and with almost the same path. Clearly, the Interferogram obtained by the MS analysis is affected by a resolution loss, which is however admissible for the objective of this paper (identification of slowly variant geometrical errors).

2. THE INSAR PHASE MODEL

We define in Eq. 1 the geometric contribution to the InSAR phase as the difference of distance between target and sensor positions.

$$\Delta\varphi = \frac{4\pi}{\lambda}[|S_1 - P| - |S_2 - P|] \qquad (1)$$

Where S_1 and S_2 are respectively the vector of master and slave position and P the vector which define the target position. We assume that just the slave position is affected by an error.

$$\Delta\varphi_{err} = \frac{4\pi}{\lambda}[|S_2 - P| - |S_2^n - P^n|] \qquad (2)$$

Where S_2^n and P^n are respectively the known vector position of the slave and the target, both altered by errors.
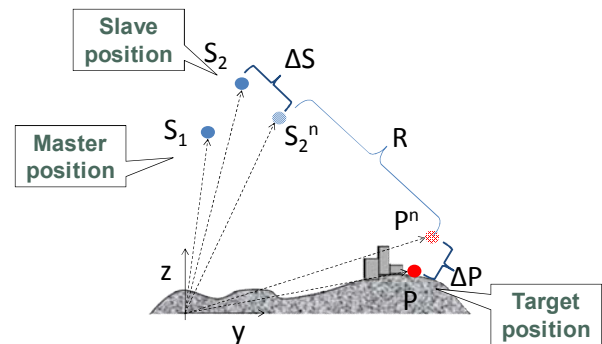

Figure 1. Geometry of the problem.

The geometric errors are the following vectors also displayed in the Fig. *1*:

$$\Delta S = S_2 - S_2^n = [\delta X, \delta Y, \delta Z]$$
$$\Delta P = P - P^n = [\delta x, \delta y, \delta z] \qquad (3)$$

According to the problem geometry just defined we can obtain the InSAR phase error contribution:

$$\Delta \varphi_{err} = \frac{4\pi}{\lambda}[-sin(\Theta_L) \cdot \delta Y + cos(\Theta_L) \cdot \delta Z \qquad (4)$$
$$-sin(\Theta_L) \cdot \delta y + cos(\Theta_L) \cdot \delta z]$$

Where Θ_L is the look angle. Eq. 4 connects InSAR phase artifacts to the geometric error for each acquisition time of the Interferogram along the orbit. In this relationship the DEM errors and the errors due to the orbit unknown motion are well identifiable. In this paper we focus on the effects of the baseline errors and their variation along the along track direction. As first step of this research we verified the match between the Eq. 4 and the simulated data. The data used in this analysis have been simulated by a typical set of parameters of TSX stripmap acquisition, and the simulated orbital errors are just constant or at most linear in the along track direction.
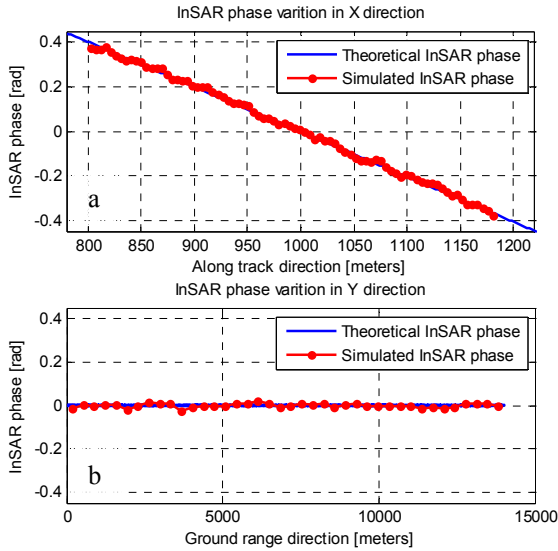

Figure 2. InSAR phase in along track direction (linear orbit error).

Fig. *2* displays the match between the InSAR phase as obtained using a numerical simulation and evaluated through Eq. 4, in the particular case of a linear variation of baseline error in the along track direction (0.5 cm/Km). In particular Fig. *2*.a and Fig. *2*.b expose respectively the phase artifacts behaviour in along track and ground range direction.

Eq. 4 defines the theoretical model of InSAR phase but does not take into account the APS contribution, which would bias the phase measurements in the case of a real data-set

3. THE MS PHASE MODEL

The multi-squint technique exploits the correspondence between the azimuth frequency and the squint angle in order to observe the same target with a slightly different angle. The MS phase is the phase of the complex conjugate product performed between the two interferograms each obtained combining master and slave acquisition with the same looks. Throughout this paper, a "look" is defined as each one of the two not overlapping sub-bands in azimuth spectrum of the full band images, as illustrated in Fig. 3. The algorithm to compute the MS phase will be detailed in this section.

The small difference in terms of the target observation position between the two looks entails that:

- the MS phase is more sensitive to orbital error variations along azimuth than the InSAR phase.
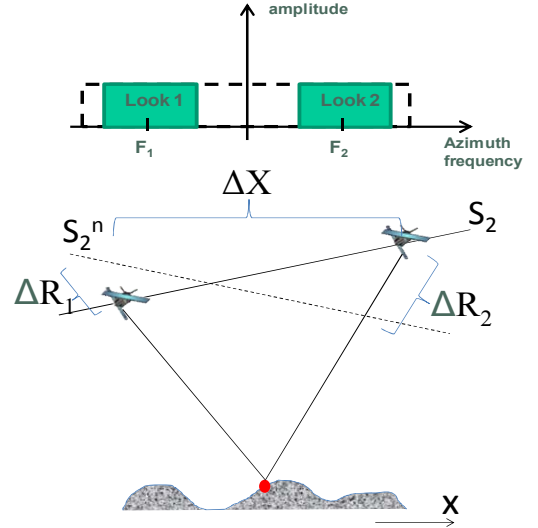- the MS phase is less sensitive to the APS and target phase contribution.

Figure 3. The geometry of the MS analysis.

The procedure to obtain the MS phase is the same already described in [9], but we summarize here the main steps of the algorithm:

1. For both the master and slave image, two sub-looks (Look 1 and 2 in Fig. 3) in azimuth frequency are generated.
2. A first couple of interferograms are computed as follows:
   a. $Interf_{Look1} = Master_{Look1} \cdot (Slave_{Look1})^*$
   b. $Interf_{Look2} = Master_{Look2} \cdot (Slave_{Look2})^*$
   Where $(...)^*$ is the complex conjugate operator.
3. In the end we compute the MS phase as complex-conjugate of the two interferograms generated in the previous step.

Hereinafter the theoretical formulation of MS phase (considering just the main contributions) results in

$$\partial \Delta \varphi = \frac{4\pi}{\lambda} \cdot 2 \cdot \tan\left(asin\left(\frac{F_{Look} \cdot \lambda}{2 \cdot V_{sat}}\right)\right) \cdot \qquad (5)$$

$$\left[\delta X + \frac{2R}{\Delta X} \cdot (-\sin(\theta_L) \cdot \delta Y + \cos(\theta_L) \cdot \delta Z) \right]$$

Where $2 \cdot F_{Look}$ is the frequency separation between the two looks (F_1 and F_2 are equal to 1/3 of the azimuth bandwidth), V_{sat} the sensor velocity, δX the mis-registration and R the slant range. In Eq. 5 we keep just two contributions for the geometric error:

- **δX** : the residual mis-registration between master and slave [9].
- **$-\sin(\theta_L) \cdot \delta Y + \cos(\theta_L) \cdot \delta Z = \Delta R$** : this contribution take into account how the parallel component of the vector baseline error change in along track direction [5]. The total baseline error ΔR is the sum of orbit error for the two sub-looks as displayed in Fig. 3 ($\Delta R = \Delta R_1 + \Delta R_2$).

By analysis of Eq. 5, the following considerations can be made:

- The MS phase is sensitive to a baseline error which varies in along track direction.
- A linear variation (in along track direction) of the baseline error leads to a linear MS phase in ground range direction and to a constant MS phase in along track direction, as it is shown in (Fig. *4*.b) and in (Fig. *4*.a) respectively.
- A residual mis-registration in azimuth direction (if constant in the slave) causes a constant MS phase in both direction (Fig. *5*).
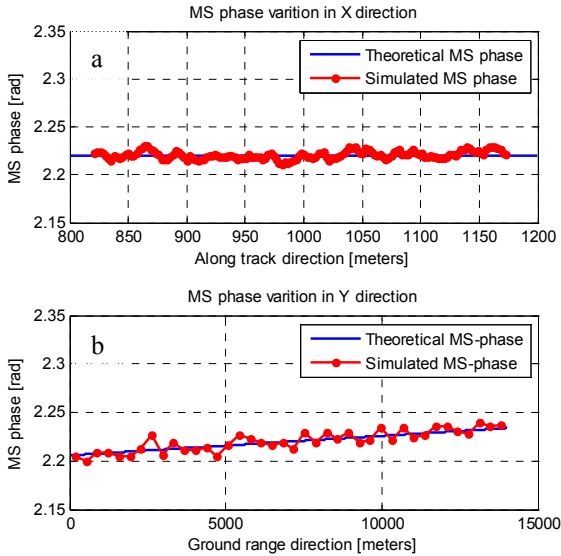

Figure 4. MS phase: theoretical and simulated results (linear orbit error: 0.5cm/Km).
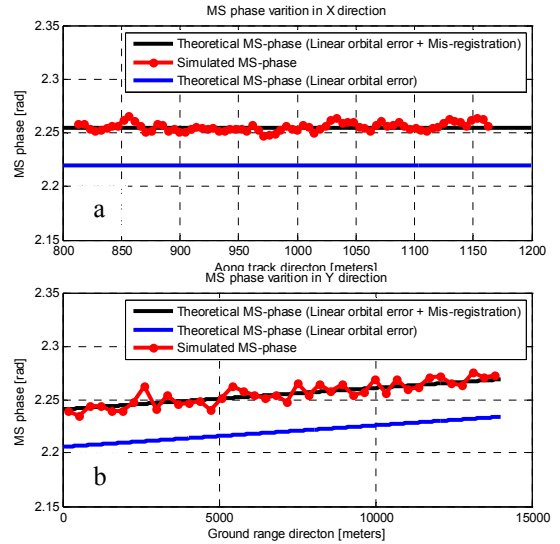

Figure 5. MS phase: theoretical and simulated results (linear orbit error: 0.5cm/Km + residual mis-registration: 0.02 pixels).

Similarly to the InSAR model, that has been defined in the previous section, the MS phase model here presented does not take into account the APS. We will show in the next section the less sensitivity of the MS phase to the atmospheric phase delay.

4. APS EFFECTS ON THE MS PHASE

Usually the dominant atmospheric contribution to the InSAR phase is due to the liquid water content (LWC). Water vapor is mainly contained in the first 2 Km above the ground [10], but a high level of LWC (> 2 g/m^3) can also occur over 10 Km of altitude in case of cumulonimbus in the scene [11][12]. Cumulonimbus is the kind of cloud with the highest level of LWC and it extends vertically more than 8 Km, so that its extension is greater than the other kinds of clouds. In order to understand the cumulonimbus geometry we have to define the fundamental building block of this kind of cloud, which is called cell. The cell is defined as a region of the cloud with spatial and temporal coherency and it has usually a diameter larger than 1 Km.
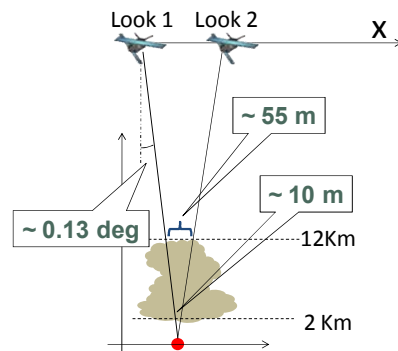

Figure 6. The geometry of the MS analysis for a spaceborne system.

According to the cumulonimbus structure and the geometry in Fig. *6* we can say that the distance between the two paths, in the troposphere, is much shorter than the spatial coherency of clouds. Consequently we can expect that the multi-squint phase is less affected by the APS than the InSAR phase.
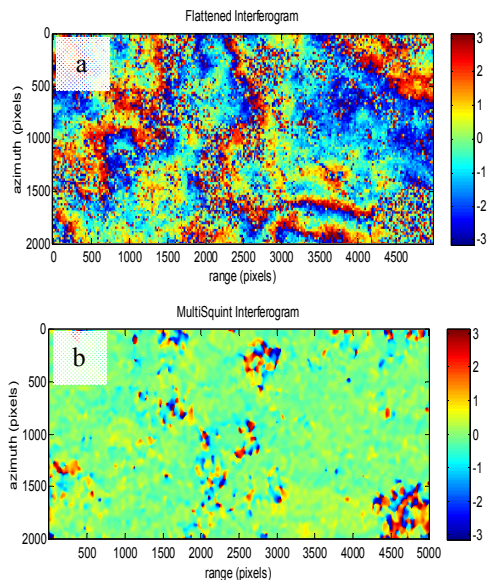

Figure 7. MS analysis on TSX data affected by a strong APS.

The results of MS analysis performed on an interferometric pair acquired by the TSX is illustrated in Fig. *7*. The flattened interferogram (Fig. *7*.a) exhibits wrapped phase fringes due to a strong APS (probably due to a storm), whereas in the MS interferogram (Fig. *7*.b) the atmospheric contributions are almost completely removed, as it was expected by the considerations drawn above.

5. CONCLUSIONS

Even a small orbital error (a few millimeters per kilometer) leads to artifacts on the interferogram.
Such artifacts are hard to separate from those due to the atmospheric delay, which also affects the InSAR phase. In this paper squint angle diversity was proposed as a solution to separate orbital errors from APS. Theoretical analyses and preliminary results on TSX data appear to support the validity of this concept. Current researches are focused on concept validation with other data and on the development of an operational procedure to estimate orbital errors.

6. REFERENCES

1. Scharroo, R., Visser, P.: Precise orbit determination and gravity field improvement for the ERS satellites. Journal of Geophysical Research: Oceans (1978--2012) 103(C4), 8113-8127 (1998)

2. Covello, F., Battazza, F., Coletta, A., Lopinto, E., Fiorentino, C., Pietranera, L., Valentini, G., Zoffoli, S.: COSMO-SkyMed an existing opportunity for observing the Earth. Journal of Geodynamics 49(3), 171-180 (2010)

3. Wermuth, M., Hauschild, A., Montenbruck, O., Jäggi, A.: TERRASAR-X RAPID AND PRECISE ORBIT DETERMINATION. (2007)

4. Gatti, G., Tebaldini, S., Mariotti D'Alessandro, M., Rocca, F.: Algae: A fast algebraic estimation of interferogram phase offsets in space-varying geometries. Geoscience and Remote Sensing, IEEE Transactions on 49(6), 2343-2353 (2011)

5. Reigber, A., Prats, P., Mallorqui, J. J.: Refined Estimation of Time-Varying Baseline Errors in Airborne

6. Pepe, A., Berardino, P., Bonano, M., Euillades, L. D., Lanari, R., Sansosti, E.: SBAS-Based Satellite Orbit Correction for the Generation of DInSAR Time-Series: Application to RADARSAT-1 Data. Geoscience and Remote Sensing, IEEE Transactions on 49(12), 5150-5165 (dec. 2011)

7. Capkovà, I.: Satellite Orbit Errors and Their influence on Interferograms. Master's thesis, Prague (2005)

8. Goldstein, R.: Atmospheric limitations to repeat-track radar interferometry. Geophysical research letters 22(18), 2517-2520 (1995)

9. Scheiber, R., Moreira, A.: Coregistration of interferometric SAR images using spectral diversity. Geoscience and Remote Sensing, IEEE Transactions on 38(5), 2179-2191 (2000)

10. Ding, X.-l., Li, Z.-w., Zhu, J.-j., Feng, G.-c., Long, J.-p.: Atmospheric effects on InSAR measurements and their mitigation. Sensors 8(9), 5426-5448 (2008)

11. Cotton, W., Bryan, G., van den Heever, S.: Cumulonimbus Clouds and Severe Convective Storms. International Geophysics 99, 315-454 (2011)

12. Kalinin, N., Smirnova, A.: Determination of liquid water content and reserve of cumulonimbus cloudiness from meteorological radar information. Russian Meteorology and Hydrology 36(2), 91-101 (2011)

13. Closa, J.: The Influence of Orbit Precision in the Quality of ERS SAR Interferometric Data. Tech. rep., ESA (1998)